Theoretical analysis of deuteron-induced reactions and development of deuteron nuclear database

Shinsuke NAKAYAMA
Nuclear Data Center, Japan Atomic Energy Agency
2-4 Shirakata, Tokai-mura, Naka-gun, Ibaraki 319-1195, Japan
Email: nakayama.shinsuke@jaea.go.jp

Intensive fast neutron sources using deuteron accelerators have been proposed for various applications. Toward evaluation of deuteron nuclear data, we have developed a code system dedicated for deuteron-induced reactions, named DEURACS. In this paper, we present the results of theoretical analysis for (*d*,*xn*) reactions with DEURACS and discuss how important it is to consider the breakup processes for accurate prediction of deuteron-induced reaction cross sections. Moreover, we have recently developed deuteron nuclear database JENDL/DEU-2020 by employing DEURACS. The validation results of JENDL/DEU-2020 are also presented.

1. Introduction

Since deuteron is a weakly bound system whose binding energy is 2.225 MeV, it easily breaks up and emits a neutron through interaction with a target nucleus. Utilizing this property, intensive fast neutron sources using deuteron accelerators have been proposed for not only science and engineering fields [1, 2] but also medical applications [3]. In the above-mentioned accelerator-based neutron sources, (*d*,*xn*) reactions on Li, Be, or C are employed to generate neutron beams. Thus, for design studies of such neutron sources, accurate and comprehensive nuclear data of deuteron-induced reactions especially on Li, Be, and C isotopes are indispensable.

Under these circumstances, we have developed a code system dedicated for deuteron-induced reactions toward deuteron nuclear data evaluation. The code system was named DEURACS, and it was so far successfully applied to analyses of production of nucleons [4, 5], composite particles up to $A = 4$ [6, 7], and residual nuclei [8]. From these results, it is expected that DEURACS describes the mechanism of deuteron-induced reaction well and is suitable for completing deuteron nuclear data through interpolation and extrapolation of available experimental values. Thus, we have recently developed a deuteron nuclear database up to 200 MeV for ^{6,7}Li, ^{9}Be, and ^{12,13}C by employing DEURACS. The new database was named JENDL/DEU-2020 [9] as one of the series of JENDL special-purpose files.

In this paper, we first present the brief overview of DEURACS and the results of analysis for the Li(*d*,*xn*) reactions as an example of the theoretical analysis with DEURACS. Through the analysis, we discuss how important it is to consider the breakup processes of incident deuteron. Next, the outline of JENDL/DEU-2020 is given and then the validation results of JENDL/DEU-2020 through comparison with experimental data are presented.

2. Theoretical analysis of deuteron-induced reactions

2.1. Overview of DEURACS

DEURACS consists of several calculation codes based on theoretical models to describe each

reaction process characteristic of deuteron-induced reactions. In the following, we briefly outline the theoretical models and methods in DEURACS to calculate the double differential cross section (DDX) of (*d*,*xn*) reaction that is a fundamental quantity in terms of neutron production. More details about the models and methods in DEURACS are described for (*d*,*xn*) reaction in Ref. [9] and for other reactions in Refs. [6-8].

In DEURACS, the DDXs of (*d*,*xn*) reactions are expressed by incoherent summation of the following components:

$$\frac{d^2\sigma_{(d,xn)}}{dEd\Omega} = \frac{d^2\sigma_{\mathrm{EB}}}{dEd\Omega} + \frac{d^2\sigma_{\mathrm{NEB}}}{dEd\Omega} + \frac{d^2\sigma_{\mathrm{PE+CN}}}{dEd\Omega}, \quad (1)$$

where $d^2\sigma_{\mathrm{EB}}/(dEd\Omega)$, $d^2\sigma_{\mathrm{NEB}}/(dEd\Omega)$, and $d^2\sigma_{\mathrm{PE+CN}}/(dEd\Omega)$ correspond to the DDXs for elastic breakup, nonelastic breakup, and pre-equilibrium and compound nucleus processes, respectively.

First, the elastic breakup component is directly calculated by the continuum-discretized coupled-channels (CDCC) method [10]. Next, the nonelastic breakup component is calculated by the Glauber model with the noneikonal approach described in Ref. [11]. In this approach, the eikonal *S* matrices used in the Glauber model are replaced by the quantum *S* matrices given by the optical model calculations. However, the Glauber model cannot properly calculate the (*d*,*n*) transfer reactions to the specific bound states in the residual nucleus, which is a part of nonelastic breakup. To deal with this problem, we separately calculate the transfer reaction by a conventional zero-range distorted wave Born approximation (DWBA) using the DWUCK4 code [12].

In addition to the breakup processes, the pre-equilibrium and the compound nucleus processes are calculated using the two-component exciton model and the Hauser-Feshbach model implemented in the CCONE code [13]. In deuteron-induced reactions, three types of composite nuclei can be formed by the absorption of either neutron or proton in the incident deuteron or the incident deuteron itself. In DEURACS, a calculation taking these effects into account is performed by combining the Glauber model and the models in CCONE. Moreover, DEURACS was recently modified to take into account the contribution of sequential particle decay from discrete levels in residual light nuclei [e.g., ^{9}Be(*Ex* = 2.43 MeV)] and unstable ones (e.g., ^{5}He) [9].

2.2. Theoretical analysis of (*d*,*xn*) reactions

To understand the relations among the reaction processes, we first perform a component-by-component analysis of DDXs of (*d*,*xn*) reactions. The results for the Li(*d*,*xn*) reactions at 40 MeV are presented in Figure 1. The DDXs of the ^{7}Li(*d*,*xn*) reactions calculated with DEURACS are decomposed into three components as expressed in the right-hand side of Equation (1). To make the analysis clearer, the target in the calculation is assumed to be 100% ^{7}Li. In the figure, each component and the sum of the three components are shown and compared with the experimental data [14]. Note that the experimental data are those for natural lithium (92.5% ^{7}Li and 7.5% ^{6}Li). As presented in the figure, the sums of the three components well reproduce both the shape and magnitude of the experimental data regardless of the emission angles.

The sharp peak observed around 50 MeV at 0° is attributed to the (*d*,*n*) transfer reaction, which is a part of nonelastic breakup. The experimental small peak seen around 40 MeV at 0° is a contribution from the ^{6}Li(*d*,*n*)^{7}Be transfer reaction, which is not considered in the calculation presented in Figure 1. As for the broad peaks seen around half the deuteron incident energy at forward angles, they are formed by the breakup processes, namely, elastic and nonelastic breakup. The nonelastic breakup component is

dominant at 0° but it has a stronger angle dependence than the elastic breakup component, and consequently the former is smaller than the latter at 30°. This result demonstrates that it is necessary to consider the two breakup components for the accurate prediction of the DDXs of the (*d,xn*) reaction at various angles.

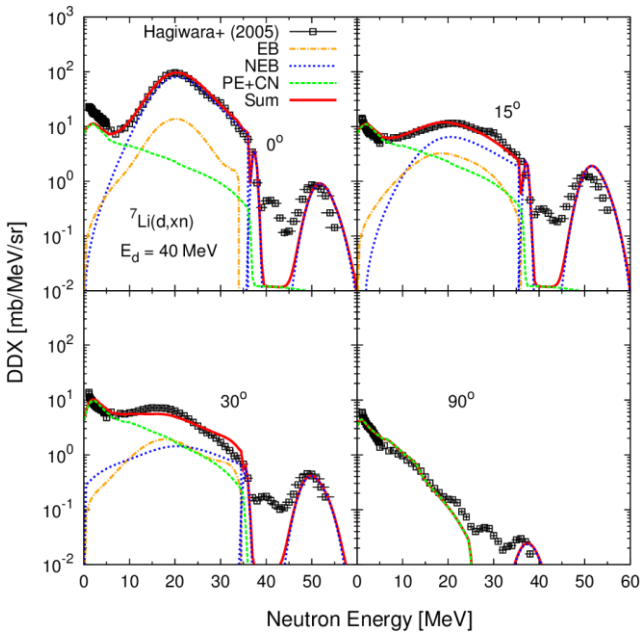

Figure 1. Calculated and experimental DDXs for the Li(*d,xn*) reactions at 40 MeV.
The number at the top of each plot denotes the emission angle.
The target in the calculation is ^{7}Li but that in the experiment is natural lithium.

On the other hand, almost all of low-energy components below 10 MeV are due to the pre-equilibrium and compound nucleus processes. Especially at 90°, the breakup components become very small and almost all spectra are explained by the contributions from the pre-equilibrium and compound nucleus processes. This indicates that the calculation method taking into account the formation of three types of composite nuclei and the particle decay from discrete levels works well.

3. Development of deuteron nuclear database

3.1. Outline of JENDL/DEU-2020

Based on the evaluation results employing DEURACS, we have developed JENDL/DEU-2020, the deuteron nuclear database for ^{6,7}Li, ^{9}Be, and ^{12,13}C at incident energies up to 200 MeV [9]. JENDL/DEU-2020 is compiled according to the ENDF-6 format. In addition to the original ENDF-6 formatted files, we have developed application libraries based on JENDL/DEU-2020 for use in the Monte Carlo transport calculation codes such as MCNP [15] and PHITS [16]. An ACE format file is available in MCNP but the present version of PHITS (version 3.20) cannot treat the ACE file for deuteron. To deal with this problem, we have developed ACE formatted files for MCNP and "Frag-Data" formatted ones for PHITS, respectively. Frag-Data is the format uniquely defined in the PHITS code. The details about the two application libraries are described in Ref. [9].

3.2. Validation results of JENDL/DEU-2020

As an example of the validation results of JENDL/DEU-2020, those for the DDXs of the (*d,xn*)

reactions on natural lithium are illustrated in Figure 2. In the figure, the calculated and experimental DDXs at 0° are compared for the incident energies up to 200 MeV. Experimental data are taken from Refs. [14, 17-19]. As for JENDL/DEU-2020, we obtained the DDXs from the MCNP calculation for a thin lithium target using the ACE file of JENDL/DEU-2020. This is because the effect of deuteron energy loss in the target is seen in the experimental data. The thickness of the target is set to be the same as that used in each experiment. For comparison, we also present the calculation results with the models implemented in the PHITS code. In the PHITS calculation, the approach combining the Intra-Nuclear Cascade of Liège (INCL) [20] and DWBA proposed by Hashimoto et al. [21] is adopted. The values stored in the deuteron sub-library of TENDL-2017 [22] are also plotted.

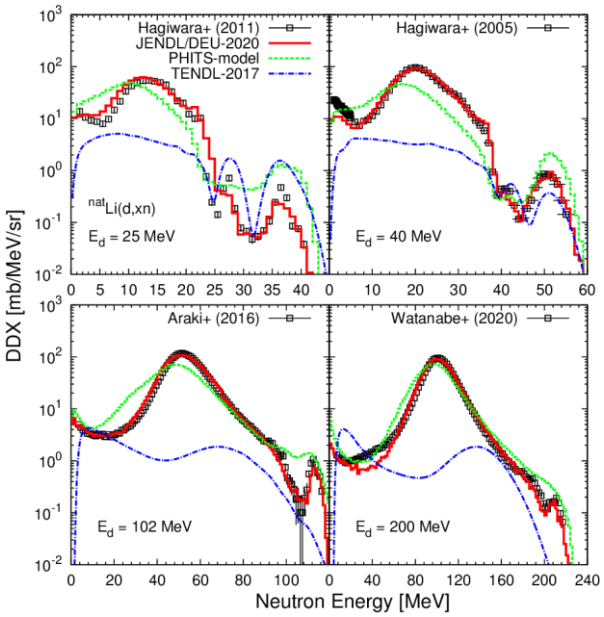

Figure 2. Calculated and experimental DDXs at 0° for the ^{nat}Li(*d*,*xn*) reactions. Incident energies are 25, 40, 102, and 200 MeV.

As shown in the figure, the calculation results based on JENDL/DEU-2020 reproduce experimental data better than the results with the models in PHITS and the values of TENDL-2017 in a wide range of incident energies. As for the calculation with the models in PHITS, the magnitudes and positions of the broad peaks around half the deuteron incident energies are different from the experimental ones especially in the low incident energies. On the other hand, TENDL-2017 underestimates the experimental values considerably at all incident energies. This indicates that the empirical model by Kalbach [23] adopted in TENDL to evaluate the breakup components does not work well for light target such as lithium.

To evaluate the results in Figure 2 more quantitatively, we calculate a relative deviation from experimental value by the following equation:

$$s = \frac{\sum \left| \sigma_i^{exp.} - \sigma_i^{calc.} \right| \Delta E_i}{\sum \sigma_i^{exp.} \Delta E_i}, \tag{2}$$

where $\sigma_i^{exp.}$ is experimental DDX at *i*-th neutron energy point, $\sigma_i^{calc.}$ is calculated DDX at the energy point corresponding to $\sigma_i^{exp.}$, and ΔE_i is energy bin of $\sigma_i^{exp.}$. Figure 3 illustrates the deviations obtained from the three calculations presented in Figure 2.

Since TENDL-2017 significantly underestimates the experimental DDXs, the deviations are almost 100% in each incident energy. As for the models in PHITS, the deviations become smaller as the incident

energy increases. This is because the picture of the INC model becomes more appropriate as the incident energy increases. The deviations obtained from JENDL/DEU-2020 are less than 15% for all incident energies. In addition to that, we have confirmed that the prediction accuracy of JENDL/DEU-2020 for beryllium and carbon targets is as good as that for lithium target [9]. From these results, it is expected that neutron production data of JENDL/DEU-2020 are reliable and it makes a large contribution to design studies of neutron sources with deuteron accelerator.

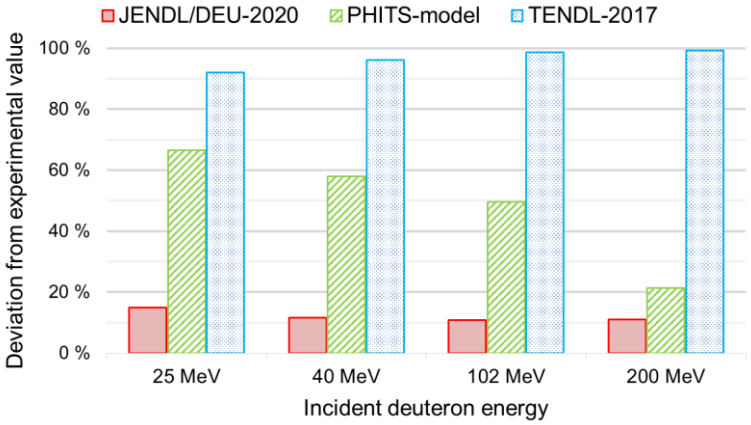

Figure 3. Relative deviations from experimental values defined by Equation (2) in terms of DDXs at 0° for the ^{nat}Li(*d*,*xn*) reactions.

4. Summary

We have presented the results of theoretical analysis for the Li(*d*,*xn*) reactions with DEURACS, which is the code system dedicated for deuteron-induced reaction we have developed. From the analysis, it has been shown that consideration of the breakup processes is essentially important for accurate prediction of deuteron-induced reaction cross sections. Based on the evaluation results employing DEURACS, we have developed JENDL/DEU-2020, the deuteron nuclear database for ^{6,7}Li, ^{9}Be, and ^{12,13}C at incident energies up to 200 MeV. From the comparison with experimental data, it has been demonstrated that the calculation results based on JENDL/DEU-2020 reproduces the measured neutron production data well at incident energies from a few tens of MeV to 200 MeV. JENDL/DEU-2020 is expected to make a large contribution to diverse design studies of deuteron accelerator neutron sources.

References

1) Ledoux X, Aiche M, Avrigeanu M, et al. The neutrons for science facility at SPIRAL-2. Nucl Data Sheets. 2014;119:353-356.
2) Moeslang A, Heinzel V, Matsui H, et al. The IFMIF test facilities design. Fusion Eng Des. 2006;81:863-871.
3) Nagai Y, Hashimoto K, Hatsukawa Y, et al. Generation of radioisotopes with accelerator neutrons by deuterons. J Phys Soc Jpn. 2013;82:064201.
4) Nakayama S, Watanabe Y. Systematic investigation of spectroscopic factors from (*d*,*p*) reactions for deuteron nuclear data evaluation. J Nucl Sci Technol. 2016;53:89-101.
5) Nakayama S, Kouno H, Watanabe Y, et al. Theoretical model analysis of (*d*,*xn*) reactions on ^{9}Be and ^{12}C at incident energies up to 50 MeV. Phys Rev C. 2016;94:014618.
6) Nakayama S, Kouno H, Watanabe Y, et al. Development of a code system DEURACS for

theoretical analysis and prediction of deuteron-induced reactions. EPJ Web Conf. 2017;146:12025.
7) Nakayama S, Iwamoto O, Watanabe Y. Consistent description of light composite particle emission in deuteron-induced reactions. Phys Rev C. 2019;100:044603.
8) Nakayama S, Furutachi N, Iwamoto O, et al. Role of breakup processes in deuteron-induced spallation reactions at 100–200 MeV/nucleon. Phys Rev C. 2018;98:044606.
9) Nakayama S, Iwamoto. O, Watanabe Y, et al. JENDL/DEU-2020: deuteron nuclear data library for design studies of accelerator-based neutron sources. J Nucl Sci Technol. 2021;DOI: 10.1080/00223131.2020.1870010.
10) Yahiro M, Ogata K, Matsumoto T, et al. The continuum discretized coupled-channels method and its applications. Prog Theor Exp Phys. 2012;2012:01A206.
11) Ye T, Hashimoto S, Watanabe Y, et al. Analysis of inclusive (*d*,*xp*) reactions on nuclei from ^{9}Be to ^{238}U at 100 MeV. Phys Rev C. 2011;84:054606.
12) Kunz P, Rost E. The distorted-wave Born approximation. In: Computational nuclear physics 2. Springer; 1993. p. 88-107.
13) Iwamoto O, Iwamoto N, Kunieda S, et al. The CCONE code system and its application to nuclear data evaluation for fission and other reactions. Nucl Data Sheets. 2016;131:259-288.
14) Hagiwara M, Itoga T, Kawata N, et al. Measurement of neutron emission spectra in Li(*d*,*xn*) reaction with thick and thin targets for 40-MeV deuterons. Fusion Sci Technol. 2005;48:1320-1328.
15) Goorley T, James M, Booth T, et al. Initial MCNP6 release overview. Nucl Technol. 2012;180:298-315.
16) Sato T, Iwamoto Y, Hashimoto S, et al. Features of particle and heavy ion transport code system (PHITS) version 3.02. J Nucl Sci Technol. 2018;55:684-690.
17) Hagiwara M, Itoga T, Oishi T, et al. Experimental studies of neutron emission spectra in Li(d,xn) reactions for IFMIF. J Nucl Mater. 2011;417:1284-1287.
18) Araki S, Watanabe Y, Kitajima M, et al. Systematic measurement of double-differential neutron production cross sections for deuteron-induced reactions at an incident energy of 102 MeV. Nucl Instrum Methods A. 2017;842:62-70.
19) Watanabe Y, Sadamatsu H, Araki S, et al. Study of the Li(*d*,*xn*) reaction for the development of accelerator-based neutron sources. EPJ Web Conf. 2020;239:20012.
20) Boudard A, Cugnon J, David JC, et al. New potentialities of the Liège intranuclear cascade model for reactions induced by nucleons and light charged particles. Phys Rev C. 2013;87:014606.
21) Hashimoto S, Iwamoto Y, Sato T, et al. New approach to description of (*d*,*xn*) spectra at energies below 50 MeV in Monte Carlo simulation by intra-nuclear cascade code with distorted wave Born approximation. Nucl Instrum Methods B. 2014;333:27-41.
22) Koning A, Rochman D, Sublet JC, et al. TENDL: complete nuclear data library for innovative nuclear science and technology. Nucl Data Sheets. 2019;155:1-55.
23) Kalbach C. Preequilibrium reactions with complex particle channels. Phys Rev C. 2005;71:034606.

Acknowledgements

The author is grateful to O. Iwamoto, Y. Watanabe, and K. Ogata for fruitful discussions. This work was partially funded by JSPS KAKENHI Grant Number 19K15483.